Journal of
Plankton Research

plankt.oxfordjournals.org

J. Plankton Res. (2016) 38(5): 1302–1316. First published online August 3, 2016 doi:10.1093/plankt/fbw053

Salinity effects on growth and toxin production in an *Alexandrium ostenfeldii* (Dinophyceae) isolate from The Netherlands

HELGE MARTENS[1], DEDMER B. VAN DE WAAL[2], KAREN M. BRANDENBURG[2], BERND KROCK[1] AND URBAN TILLMANN[1]*

[1]ALFRED WEGENER INSTITUTE HELMHOLTZ CENTRE FOR POLAR AND MARINE RESEARCH, AM HANDELSHAFEN 12, 27570 BREMERHAVEN, GERMANY AND [2]DEPARTMENT OF AQUATIC ECOLOGY, NETHERLANDS INSTITUTE OF ECOLOGY, P.O. BOX 50, 6700 AB WAGENINGEN, THE NETHERLANDS

*CORRESPONDING AUTHOR: urban.tillmann@awi.de

Received April 26, 2016; accepted June 20, 2016

Corresponding editor: John Dolan

Alexandrium ostenfeldii is among the most intensely studied marine planktonic dinophytes and in the last few years blooms have become a recurrent phenomenon mainly in brackish coastal waters. Since 2012, *A. ostenfeldii* recurs annually in the Ouwerkerkse Kreek, a Dutch brackish water creek discharging into an estuary with large stocks of mussels, oysters and cockles. The creek is characterized by highly dynamic abiotic conditions, notably salinity. Here, we investigated the impacts of salinities ranging from 3 to 34 on growth and toxin content of an *A. ostenfeldii* isolate from the creek. Our results demonstrate a broad salinity tolerance of the Dutch *A. ostenfeldii* population, with growth rates from 0.13 to 0.2 d^{-1} over a salinity range from 6 to 34. Highest paralytic shellfish toxin and cyclic imine toxin cell quotas were observed for the lowest and highest salinities, and were associated with increases in cell size. Lytic activity was highest at the lowest salinity, and was 5-fold higher in the cell-free supernatants compared to cell extracts. Together our results demonstrate a tight coupling between salinity and *A. ostenfeldii* growth rate, cell size and toxin synthesis, which may have consequences for the seasonal dynamics of bloom toxicity.

KEYWORDS: harmful algal blooms; salinity effects; growth; PSP-toxins; spirolides; gymnodimines; lytic activity

INTRODUCTION

The marine dinophycean species *Alexandrium ostenfeldii* (including *A. peruvianum*, Kremp *et al.*, 2014) is globally distributed in temperate waters and is known to produce various bioactive substances including lytic compounds (Tillmann *et al.*, 2007) and a number of highly

potent neurotoxins, such as spirolides (SPX), gymnodimines (GYM) and paralytic shellfish poisoning toxins (PST) (Kremp *et al.*, 2014). PST are a group of neurotoxic compounds, including saxitoxin (STX), neosaxitoxin (NEO), gonyautoxins (GTX), and their *N*-sulfocarbamoyl variants, the B- and C-toxins (Shimizu, 1996; Anderson *et al.*, 2012). Both GYM and SPX are part of a heterogeneous group of toxins sharing an imine moiety as bioactive pharmacophore causing spiroimine shellfish poisoning (Cembella and Krock, 2008). Up to now, spiroimines within *Alexandrium* have only been found in *A. ostenfeldii*. Although *A. ostenfeldii* often occurs at low background concentrations and is outnumbered by co-occurring phytoplankton, high concentrations of monospecific *A. ostenfeldii* blooms can occur. Such blooms have been reported mainly from almost brackish coastal systems such as the Narragansett Bay and the New River Estuary on the US east coast (Borkman *et al.*, 2012; Tomas *et al.*, 2012), or in the Baltic Sea off Finland (Hakanen *et al.*, 2012).

In the last years, reoccurring harmful algal bloom-events caused by *A. ostenfeldii* have also been observed in the Ouwerkerkse Kreek, located in the south-western part of The Netherlands. This is a shallow brackish water creek used as a drainage channel for local agriculture. A dense bloom of *A. ostenfeldii* was first observed here in 2012 (Burson *et al.*, 2014). Water analyses during the bloom revealed considerable concentrations of STX and its analogues, and *A. ostenfeldii* was found to be the most dominant species in the phytoplankton assemblage (Burson *et al.*, 2014). In the following year, a dense *A. ostenfeldii* bloom of over 4000 cells mL^{-1} was again recorded (Van de Waal *et al.*, 2015). In a first analysis of the Dutch *A. ostenfeldii* population, Van de Waal *et al.* (2015) characterized the bloom population as a member of the *A. ostenfeldii* complex Group 1 (see also Kremp *et al.*, 2014). *A. ostenfeldii* from Ouwerkerkse Kreek was found not only to produce different PST and various SPX, but also gymnodimine A and 12-methyl gymnodimine A (Van de Waal *et al.*, 2015). This toxin composition is most similar to two isolates of *A. ostenfeldii* from the USA, which also produce PST, SPX and 12-methyl gymnodimine A (van Wagoner *et al.*, 2011; Borkman *et al.*, 2012; Tomas *et al.*, 2012).

The local hydrographic conditions in the Ouwerkerkse Kreek suggest that the Dutch *A. ostenfeldii* blooms are exposed to different salinities, which vary spatially and temporally on short term (e.g. rainfall) as well as long term (e.g. seasonality, discharge regimes). The eco-physiological impacts of such different salinities for the local *A. ostenfeldii* population are largely unknown. Both lower and higher salinities may reduce growth due to enhanced energy loss by osmoregulation, which is mainly achieved by active transport of ions in or out of the cell and by accumulation of low molecular organic solutes (Stefels, 2000). Furthermore, at lower salinities, cells may accumulate water caused by osmosis as many unicellular algae are not able to build up high intracellular turgor pressures, which implies that cells increase their cell volume as water flows in (Stefels, 2000). Indeed, cell size of *A. ostenfeldii* has been shown to change with salinity, with larger cells at both highest and lowest salinities (Jensen and Moestrup, 1997; Lim and Ogata, 2005), where larger cell sizes are associated with low growth rates. Such changes in cell size and growth may very well alter synthesis and cellular accumulation of toxins. For instance, toxin quota followed the growth optima in multiple *A. ostenfeldii* clones (Lim and Ogata, 2005; Suikkanen *et al.*, 2013), while they may also be highest at salinities unfavourable to growth (Maclean *et al.*, 2003). Besides changes in toxin quota, salinity was also shown to alter toxin composition, though responses seemed strongly strain specific (Suikkanen *et al.*, 2013). We are unaware of any study reporting the impact of salinity on lytic activity in *A. ostenfeldii*.

Comparable to many phytoplankton species, *A. ostenfeldii* generally displays a positive bell-shaped growth response to salinity, with optima close to the salinities experienced in nature (Jensen and Moestrup,1997; Suikkanen *et al.*, 2013; Salgado *et al.*, 2015), though optima are often strain specific and may vary greatly in range. For instance, various strains exhibited broad optimal ranges, indicated by minor changes in growth over salinities from, for instance, 20 to 35 or 6 to 20 (Suikkanen *et al.*, 2013), and from 6 to 20 (Lim and Ogata, 2005). Such broad salinity tolerances may be a result of highly dynamic salinities typical for coastal waters. We expect to find strong salinity fluctuations in the Ouwerkerkse Kreek during bloom development, and consequently a broad salinity tolerance of *A. ostenfeldii* isolated from this creek. Furthermore, at the lowest salinities we expect to find enhanced cell sizes due to inflow of water by osmoregulation, leading to reduced growth rates that will subsequently cause an increase in accumulation of cellular toxins. Similarly, we predict enhanced lytic activity at lower salinities due a stronger osmoregulation with lytic compounds following osmolyte excretion. To test our hypotheses, we exposed and acclimated *A. ostenfeldii* from the Ouwerkerkse Kreek to a broad range of salinities and followed growth, cellular carbon (C), nitrogen (N) and phosphorus (P), and toxin production. Specifically, we investigated putative shifts in PST- and cyclic imine toxin content and toxin composition, as well as the production of lytic compounds.

METHOD

Field sampling

An integrated water sample was taken of the upper 1 m of the water column once every 2 weeks from 12 May to 13 October 2015, and a 50 mL subsample was fixed with Lugol's iodine solution (Lugol) to a final concentration of 1%. *A. ostenfeldii* cells were counted with an inverted microscope (Olympus Vanox, Hamburg, Germany) at ×200 magnification. Counts were performed on 5 × 1 mL samples. Salinity depth profiles were taken the same days using a Hydrolab DS5 (Hach Lange GmbH, Düsseldorf, Germany), with measurements taken at every second yielding an average resolution of 8 data points per metre. Data were interpolated over depth and time using the standard option for contour graphs in SigmaPlot 12.5 (Systat Software, Inc., London, UK).

Culture

The *A. ostenfeldii* isolate OKNL21 used for this experiment was isolated in July 2013 during a bloom in the Ouwerkerkse Kreek (51°62′N, 3°99′E), The Netherlands (Van de Waal *et al.*, 2015). Cells were grown in natural seawater medium, which was prepared by mixing Antarctic seawater (salinity 34) with deionized water to prepare different salinities. Culture medium was sterile-filtered (0.2 µm VacuCap filters, Pall Life Sciences, Germany) and enriched with 1/2 strength K-medium (Keller *et al.*, 1987) that was modified by omitting the addition of ammonium ions. The pH of the culture medium was adjusted to pH 8.0 (EcoScan Series, Eutech instruments, Singapore) by adding 1 M hydrochloric acid. Stock cultures of *A. ostenfeldii* were routinely grown at a salinity of 10, a temperature of 15°C and an incoming photon flux density of 50 µmol photons m^{-2} s^{-1} on a 16:8 h light–dark cycle.

Experimental set-up

Growth experiments at different salinities were performed at 15°C and an incoming photon flux density of 80–100 µmol photons m^{-2} s^{-1} (cool-white fluorescent light) on a 16:8 h light–dark cycle. Different salinities (3, 4.5, 6, 10, 16, 22, 28, 34) were achieved by diluting Antarctic seawater (salinity 34) with deionized and purified Milli-Q water (Millipore GmbH, Eschborn, Germany). Conductivities were controlled with a SB80PC salinometer (VWR sympHony Meters, Beverly, MA, USA) and converted into salinities.

Prior to the experiment, cells were acclimated to the different salinities. Cells of a stock culture (salinity 10) were inoculated at cell densities of 500 cells mL^{-1} into media adjusted to salinities of 6, 10 and 16. During acclimation, the cell density was determined every 2–3 days. At a cell density of ~2.5 × 10^3 cells mL^{-1}, cells were diluted to 500 cells mL^{-1} to the next lower or higher salinity (e.g. cells from 16 were transferred to 22 and cells from 6 were transferred to 4.5) until stock cultures acclimated to all different salinities were available. During acclimation cultures were grown and diluted several times and spent at least six generations at the respective experimental salinities before starting the experiment.

The experiment was then started by transferring exponentially growing cells (based on consecutive cell counts of the inoculum culture) from each salinity to fresh medium at an initial cell density of 300 cells mL^{-1}. All cultures were set up in triplicates in 1 L Erlenmeyer flasks containing 600 mL of medium. Growth was followed by cell counts at every second day by taking Lugol fixed (2% final concentration) subsamples. Samples for measurements of toxins, lytic activity, elemental composition and cell size were taken once during exponential growth at a density of about 2 × 10^3 cells mL^{-1}, and once in stationary growth phase, when three consecutive cell counts showed that the population size did not increase.

Growth rate

Growth rate was calculated using cell counts obtained by an inverted microscope (Zeiss Axiovert 40C, Zeiss, Göttingen, Germany) at ×200 magnification. For each sample, a minimum of 400 cells were counted. The specific growth rate (μ, d^{-1}) for each replicate was calculated according to $N(t) = N_0 \exp[\mu t]$ by exponential regression of cell density versus time for a selected period of exponential increase (indicated in Supplementary Material, Fig. S1). Plotted growth curves for each salinity treatment were based on mean cell density of the three replicates (Supplementary Material, Fig. S1).

Cell size

To determine cell size, Lugol fixed (1% final concentration) cells were viewed under an inverted microscope (Zeiss Axiovert 200 M, Zeiss) and photographed at ×200 magnification with a digital camera (Axiovert, Zeiss). Measurements were taken using the analysis tool of the Axiovision software (Zeiss). A total of 30 cells were measured in length and width of each of the three replicate cultures. For statistical analysis, cell size data of the replicate cultures were combined yielding 90 cell length and width measures for each treatment. Cell volumes were calculated assuming a prolate spheroid as geometric cell shape.

Cellular C, N and P content

To analyse the C, N and P content of cells, duplicate samples of 30–50 mL culture each were filtered onto a glass-fibre filter (GF/C, d = 21 mm, Whatman, Maidstone, UK; pre-combusted at 500°C for 8 h). Blanks were set up in duplicate by filtering pure culture medium and elemental contents of these filters were subtracted from sample values. All filters were frozen at −20°C and stored for later elemental analysis.

Before analysis, filters were dried at 60°C for 24 h. Six pieces (d = 3 mm; A = 7 mm^2) were pierced out of the filter and folded into a thin capsule (Elemental Microanalysis, Okehampton, UK). The C and N content were determined by a FLASH 2000 organic elemental analyser (Brechbueler Incorporated, Interscience B.V., Breda, The Netherlands). Subsequently, the remaining part of the filter was used for measuring the P content. First, the samples were combusted for 30 min at 500°C, followed by a 2% persulphate digestion step for 30 min at 121°C in the autoclave. The digested samples were analysed using a QuAAtro segmented flow analyser (Seal Analytical Incorporated, Beun de Ronde, Abcoude, The Netherlands).

Analytical methods for toxin analysis

Post-column derivatization analysis of PST

Duplicate subsamples of 50 mL (exponential growth phase) or 30 mL (stationary growth phase) were harvested from each replicate culture by centrifugation (Eppendorf 5810R, Hamburg, Germany) at 3220 *g* for 10 min. Cell pellets were transferred to 2 mL microtubes, centrifuged again (Eppendorf 5415, 16 000 *g*, 5 min), and stored at −20°C until use. Cell pellets were extracted with 0.03 M acetic acid by reciprocal shaking at maximum speed (6.5 m s^{-1}) for 45 s in a FP 120 FastPrep instrument (Bio101, Thermo Savant, Illkirch, France). After centrifugation, the supernatant was spin-filtered (pore-size 0.45 mm, Millipore Ultrafree, Eschborn, Germany), the filtrate transferred into a HPLC vial (Agilent Technologies, Waldbronn, Germany) and kept at −20°C until analysis. PST analysis was performed as ion pair chromatography on an octadecyl stationary phase (C18) with two subsequent isocratic elutions: 15 min with 6 mM 1-octanesulphonic acid and 6 mM 1-heptanesulphonic acid in 40 mM ammonium phosphate, adjusted to pH 7.0 with dilute phosphoric acid and 0.75% tetrahydrofuran (THF) and then switched within 1 min to 13 mM 1-octanesulphonic acid in 50 mM phosphoric acid adjusted to pH 6.9 with ammonium hydroxide, 15% of acetonitrile and 1.5% of THF for 24 min. Post-column derivatization was performed with 10 mM periodic acid in 550 mM ammonium hydroxide and subsequently 0.75 N nitric acid; both reagents were added at a constant flow of 4 mL min^{-1}. Toxin derivatives were detected by fluorescence detection (λ_{ex} = 333 nm; λ_{em} = 395 nm). All toxins were identified and quantified against an external calibration curve containing C1/2, B1, STX, NEO, GTX-1 to 4, dcGTX-2/3 and dcSTX. These toxins were purchased from the certified reference material (CRM) programme of the National Research Council, NRC, Halifax, Canada.

Cyclic imine toxins

Duplicate 15 mL subsamples (exponential and stationary growth phase) from each replicate culture were harvested by centrifugation (Eppendorf 5810R) at 3220 *g* for 10 min. Cell pellets were transferred to 1 mL microtubes, centrifuged (Eppendorf 5415, 16 000 *g*, 5 min) and stored at −20°C until use. The supernatants were stored at −20°C for subsequent analysis of extracellular cyclic imine toxins.

Cell pellets were transferred to 2 mL microcentrifuge tubes (neoLab, Heidelberg, Germany) containing 0.5 g lysing matrix D (Thermo Savant). Subsequently, the pellets were suspended in 500 µL methanol (Merck, Darmstadt, Germany) and homogenized by reciprocal shaking at maximum speed (6.5 m s^{-1}) for 45 s in a FP 120 FastPrep instrument (Bio101, Thermo Savant). After homogenization, the samples were centrifuged (16 000 *g*, 15 min, 4°C, Centrifuge 5415R, Eppendorf) and the supernatant was transferred to a spin-filter (pore-size 0.45 mm, Millipore Ultrafree) and centrifuged for 30 s at 3220 *g*. Filtrates were transferred into HPLC vials (Agilent Technologies) and stored at −20°C.

The cyclic imine toxin measurement was performed on a 4000 Q Trap triple-quadrupole mass spectrometer (AB-Sciex, Darmstadt, Germany) with a Turbo V ion source coupled to an Agilent 1100 LC liquid chromatograph (Waldbronn, Germany). The LC was equipped with a solvent reservoir, in-line degasser (Pickering Laboratories, No. G1379A), binary pump (G1311A), refrigerated autosampler (G1329A/G1330B) and a temperature-controlled column oven (G1316A). The separation was carried out on an analytical C8 reverse phase column (50 mm × 2 mm) packed with 3 µm Hypersil BDS 120 Å (Phenomenex, Aschaffenburg, Germany) and thermostated at 20°C. The flow-rate was 0.2 mL min^{-1} and a gradient elution was performed, where eluent A consisted of water and eluent B was methanol/water (95:5, v/v), both containing 2.0 mM ammonium formate and 50 mM formic acid. Initial conditions were 5% of eluent B. After injection, a linear gradient to 100% B in 10 min was performed and followed by isocratic elution

until 20 min. Then, the eluent composition was set to initial conditions within 1 min followed by 9 min column equilibration. The total run time was 30 min. The mass spectrometric parameters were as follows: Curtain gas: 20 psi, CAD gas: medium, ion-spray voltage: 5500 V, temperature: 650°C, nebulizer gas: 40 psi, auxiliary gas: 70 psi, interface heater: on, declustering potential: 121 V, entrance potential: 10 V, exit potential: 22 V. The collision energy was 57 V for each transition. The selected reaction monitoring (SRM) transitions and characteristic group fragments of SPX are shown in Table I. Measurements were performed in the positive ion-mode and dwell times of 40 ms were used for each transition. SPX were calibrated against an external calibration curve of SPX-1 (CRM programme of the IMB-NRC, Halifax, Canada) and expressed as SPX-1 equivalents. Likewise, GYM were calibrated against an external calibration curve of gymnodimine A (CRM) and expressed as gymnodimine A equivalents. For the calibration curve, the following concentrations of SPX-1 were used: 10, 50, 100 and 1000 pg μL^{-1}. For quantifying GYM, the following concentrations of a standard solution of gymnodimine A were used: 10, 50, 500 and 1000 pg μL^{-1}. A qualitative solution of 12-methyl gymnodimine A was provided by Kirsi Harju (VERIFIN, Helsinki, Finland) and used for compound identification. Data acquisition and processing were performed with the Analyst Software (version 1.5, AB-Sciex).

Analysis of extracellular cyclic imines

The following clean-up procedure was developed and applied to culture supernatant: A C18 cartridge (Supelclean LC-18 tubes 6 mL, Supelco, Deisenhofen, Germany) was conditioned in a Visiprep Solid-Phase-Extraction vacuum manifold (Supelco) with 2 mL of methanol and equilibrated with 5 mL of deionized water. Culture supernatants were successively loaded onto the cartridges. After sample loading, cartridges were washed with 5 mL of distilled water. Elution of the cyclic imine toxins was performed with 5 mL of methanol in two steps with 2.5 mL each at a very low rate (~1 drop min^{-1}). The 5 mL eluates were evaporated in a rotary evaporator to dryness and taken up into an accurate volume of 1 mL of methanol. The extract was transferred to a HPLC glass vial and stored at −20°C for later measurement with LC-MS.

The extraction efficiency of this procedure for extracellular cyclic imine toxins had previously been determined in three independent spiking experiments: 100 mL of culture medium were mixed with 50 µL of a *A. ostenfeldii* cell extract with a known amount of cyclic imine toxins. This mixture was treated with the solid phase extraction (SPE) extraction procedure described above and the recovery rate of cyclic imine toxins was calculated.

Quantification of lytic activity

Lytic activity was quantified using a *Rhodmonas salina* lysis bioassay (Ma *et al.*, 2009; Tillmann *et al.*, 2009). For a quantitative comparison of different culture fractions, one detailed bioassay was performed using whole cell culture, cell-free supernatant and cell extracts. Therefore, 40 mL of the *A. ostenfeldii* experimental cultures grown at a salinity of 16 were sampled in exponential phase and centrifuged (5250 *g*, 15 min, Allegra X-15R Centrifuge, Beckman Coulter, Brea, CA, USA) to separate cell-free supernatant and cells. The cell pellet was extracted with 1 mL 100% methanol using an ultrasonic (Sonoplus HD70 sonotrode, Bandelin Electronics, Berlin, Germany) treatment with 50% pulse cycle and 70% amplitude for 60 s. Samples were kept on ice during ultrasonic treatment. Bioassays from whole cell culture, cell extracts and cell-free supernatant were set up as described below with one modification: we here used a culture of the target cryptophyte species *R. salina* (Kalmar culture collection, strain KAC30) that was pre-adapted from a salinity of 34 to the reduced salinity of 16 for at least 4 weeks.

*Table I: Mass transitions (*m/z*; precursor ion → fragment ion), retention times and masses of $[M+H]^+$ ions of characteristic group fragments of SPX and GYM*

				m/z			
Mass transition (*m/z*)	Common name	Qty	Retention time (min)	Group 1	Group 2	Group 3	Group 4
508 → 490	Gymnodimine A	+	11.81				
522 → 504	12-Methyl gymnodimine A	+	12.17				
692 → 164	13-Desmethyl spirolide C	+	12.76	692.7	462.5		164.2
696 → 164	Undescribed	–	12.39	696.7	464.4	292.4	164.2
708 → 180	27-Hydroxy-13-desmethyl spirolide C	–	13.06	708.3	460.2		180.3
710 → 164	Undescribed	–	12.97	710.3	462.3		164.3
720 → 164	Undescribed	–	13.29	720.7	472.6		164.2
722 → 164	Undescribed	–	13.40	722.7	472.6		164.2

+, major compound; –, minor compound.

For bioassays of the growth experiment, cells were harvested by centrifugation of 50 mL culture. The supernatant was stored at −30°C for up to 4 months before estimating extracellular lytic activity. The pellet was transferred to a 2 mL microcentrifuge tube (neoLab), centrifuged again (16 000 *g*, 5 min, Eppendorf 5415) and frozen at −20°C for later extraction. The bioassay target species *R. salina*, was maintained in full saline culture media (salinity of 34) under the same culture conditions as described before for the *A. ostenfeldii* cultures.

To avoid any salinity stress of *R. salina* treated with the different salinities of the supernatant, all supernatant samples were adjusted to a salinity of 34 prior to the bioassay by adding an adequate amount of sodium chloride (pro analysis, Merck).

Bioassays were set up in a total volume of 4 mL in 6 mL glass vials. All samples were spiked with 0.1 mL of a *R. salina* culture, which was adjusted to a concentration of 4×10^5 cells mL^{-1} to yield a final concentration of *R. salina* in the sample of 1×10^4 mL^{-1}. Samples were incubated at 15°C for 24 h in darkness. Subsequently, samples were fixed with Lugol's iodine solution (2% final concentration). Counts of intact *R. salina* cells in a sub-area of the chamber corresponding to *ca.* 600 cells in the control were carried out with an inverted microscope (Zeiss Axiovert 40 C) at ×400 magnification. All *R. salina* counts were compared to a triplicate mean of a control (incubated with culture medium) to calculate the percentage of intact *R. salina*. Bioassays were performed as a series of several dilutions of culture supernatants, *A. ostenfeldii* whole cultures or cell extracts to allow dose–response calculation. Plotting percentage of intact *R. salina* versus the logarithmic-scaled *A. ostenfeldii* concentration allowed EC_{50} values to be calculated, i.e. the *A. ostenfeldii* cell concentration yielding a 50% mortality of *R. salina*.

Calculations were carried out by Statistica (StatSoft, Tulsa, OK, USA) using a non-linear fit (Stolte *et al.*, 2002):

$$N_{\text{final}} = \frac{N_{\text{control}}}{1+((x/\text{EC}_{50})^h)}$$

where N_{final} is the final target cell concentration, N_{control} is the final target cell concentration in control samples, x is the log-transformed *A. ostenfeldii* concentration and EC_{50} and h are fit parameters. Results are presented as EC_{50} (cells mL^{-1}) within the 95% confidence interval.

Statistical analysis

A one-way ANOVA was used to analyse group means with more than three groups for statistical significance. For multiple comparisons, a Tukey's HSD *post hoc* test was performed to compare means of different treatments and assess significance of sub-group differences. Analyses were performed in SigmaPlot 12.0 (Systat Software, Inc.).

RESULTS

Field data

In 2015, *A. ostenfeldii* cells were found in the creek from mid-July until October with a distinct bloom between mid-July and mid-August with maximum population densities of nearly 800 cells mL^{-1} (Fig. 1A). During the period in which cells were detected, salinities varied in

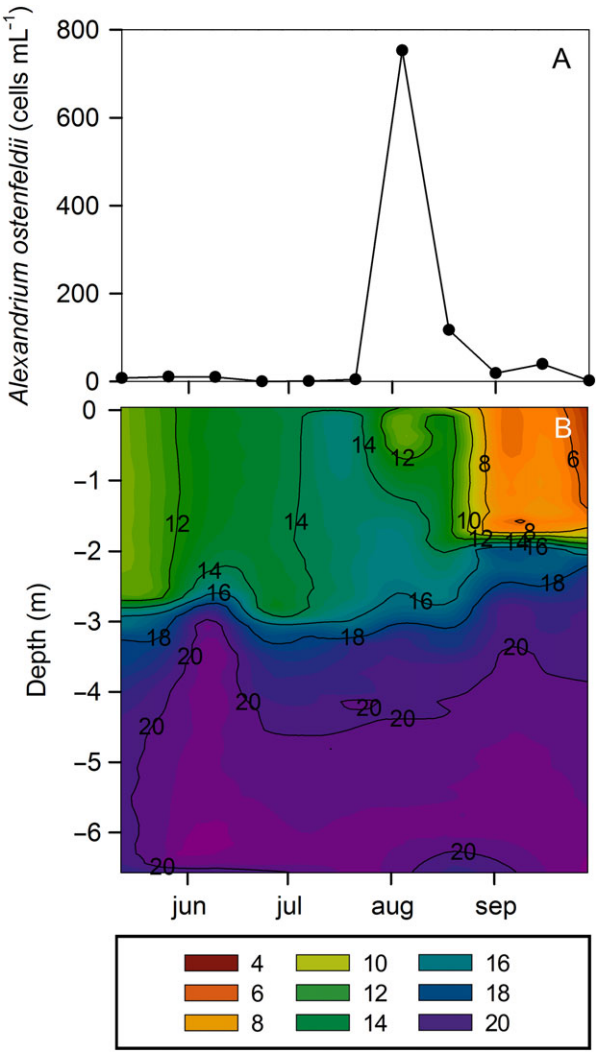

Fig. 1. Population densities of *A. ostenfeldii* in the Ouwerkerkse Kreek, The Netherlands (**A**), and salinity depth profiles (**B**) from May to October 2015.

depth and time ranging between values of around 4–20 (Fig. 1B). Over the entire year, a clear halocline was observed at a depth of 3 m, with a low salinity surface layer (salinity 8–16) on top of a higher salinity bottom layer (salinity >18). We observed a shoaling of the halocline around mid-August, due to a period of heavy rainfall (data not shown) that strongly reduced the salinity of the surface layer down to <4 (Fig. 1B). This largely coincided with the collapse of the bloom.

Experimental data

Growth

Growth was observed at salinities between 6 and 34 (Supplementary Material, Fig. S1, Fig. 2A). Although some growth was observed in a pre-culture acclimating to a salinity of 4.5, experimental cultures at this salinity did not grow (Supplementary Material, Fig. S1). Cells transferred from a salinity of 4.5 to a salinity of 3 rapidly died (data not shown). The specific growth rate (μ) ranged between 0.13 and 0.20 d^{-1}. Maximum cell concentration in the stationary phase ranged between 9×10^3 and 12×10^3 cells mL^{-1} and was comparable for all salinities (Supplementary Material, Fig. S1).

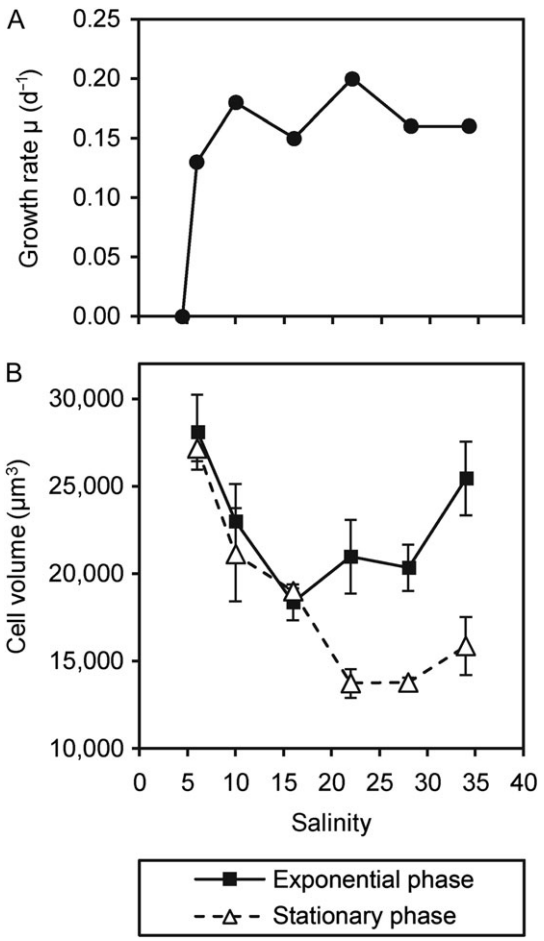

Fig. 2. Mean growth rates (**A**) and cell volumes (**B**) of *A. ostenfeldii* for different salinity treatments for triplicate cultures in the exponential and stationary growth phase ($n = 3$, ±1 SD). Error bars in A are not visible as they are smaller than the dots.

Cell volume and size

Cell width ranged from 28.8 to 35.2 μm, cell length from 31.2 to 40.6 μm within and among all treatments, and cell volume from 13 000 to 27 000 μm^3 (Supplementary Material, Tables S1 and S2). Cell volumes were smaller at intermediate salinities and increased at both lower and higher salinities, particularly in the exponential phase (Fig. 2B). At the three lowest salinities tested, cells during exponential phase had almost the same volume as cells in stationary growth. In contrast, at the three highest salinities cells in exponential growth phase were ~60% larger compared to cells in the stationary phase.

Cellular C, N and P content

The particulate carbon quota for exponential and stationary growth phase ranged from 2.0 to 4.5 ng $cell^{-1}$ (Fig. 3A, Supplementary Material, Tables S1 and S2). Among all treatments, the carbon quota was lowest at a salinity of 16 for the exponential growth phase. For the stationary growth phase, the carbon quota was lowest at a salinity of 10. For both growth phases, the cellular carbon content increased gradually and was highest at salinities of 6 and 34. The nitrogen cell quota (Fig. 3B) ranged between 0.4 and 0.6 ng $cell^{-1}$. In the exponential phase, nitrogen quota showed a tendency of a slight increase from intermediate salinities to both lower and higher salinities. Except for the salinity treatments 16 and 22, which nearly yielded the same amount of nitrogen per cell in both growth phases, the nitrogen quota was significantly higher in exponential growth phase (*t*-test, $p < 0.05$). The phosphorus quota ranged from 0.08 to 0.11 ng $cell^{-1}$ for exponential growth, and from 0.05 to 0.07 ng $cell^{-1}$ for stationary growth (Fig. 3C). In exponential phase, the phosphorus quota was lowest at a salinity of 16 and 22 and increased at higher and lower salinities. In contrast, in stationary phase the phosphorus quota was highest at salinity 16 and decreased for lower and higher salinities.

Elemental ratios of cells in exponential phase were largely comparable for all salinity treatments, ranging from 6.5 to 7.8 for C:N ratios, 11.8 to 15.0 for N:P ratios, respectively (Fig. 3D–F, Supplementary Material, Table S1). In stationary phase, C:N, C:P and N:P ratios were significantly higher for a number of treatments

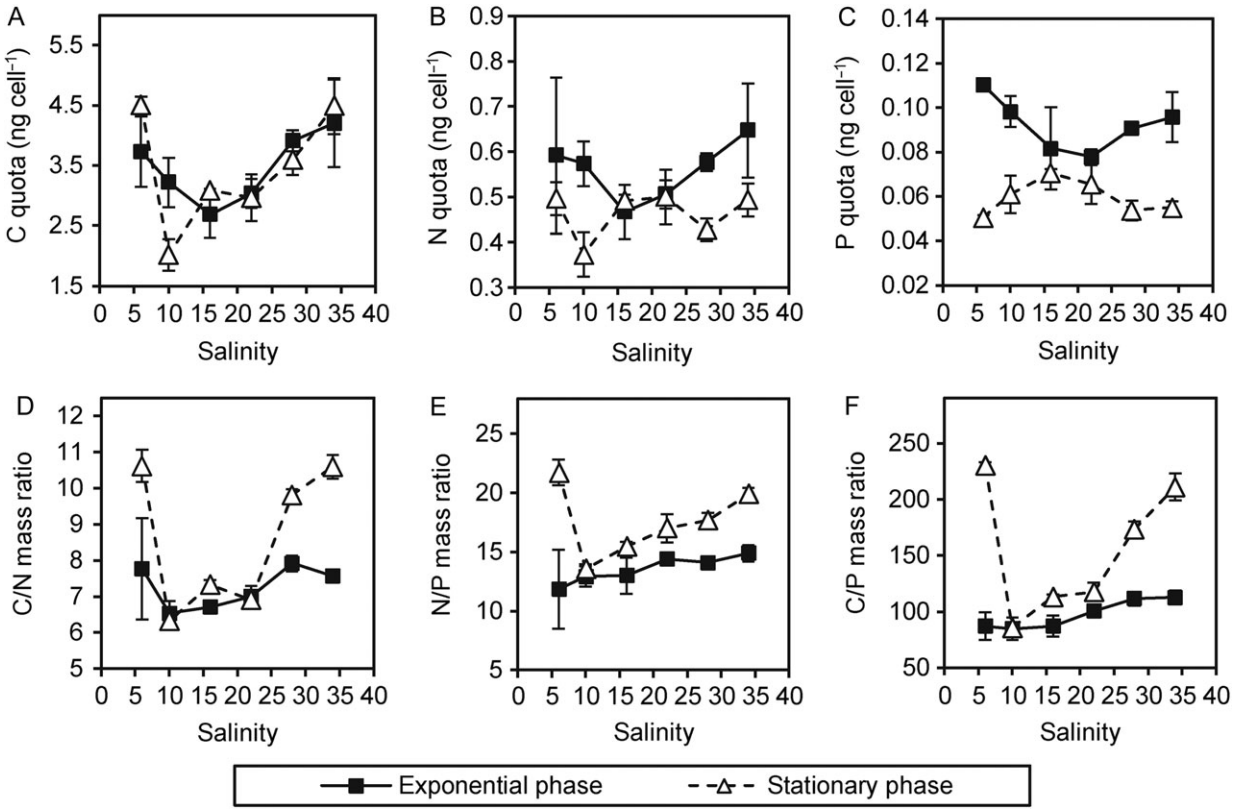

Fig. 3. Cell quotas of C, N and P (**A–C**), and elemental ratios with C:N, N:P and C:P (**D–F**) for triplicate cultures in the exponential and stationary growth phase ($n = 3$, ±1 SD).

(Fig. 3D–F, Supplementary Material, Table S2). C:N ratios of ~10 were observed for both low and high salinities, i.e. for the 6, 28 and 34 salinity treatment. For C:P ratios in the stationary phase, significantly higher values of up to 230 were observed for the 6, 28 and 34 salinity treatments. Similarly, the N:P ratio of cultures in stationary phase was most different to the exponential phase for the lowest salinity.

Toxin quota

The total PST cell quota ranged between 25.3 and 51.2 pg cell^{-1}, and between 25.4 and 39.1 pg cell^{-1} in exponential and stationary growth phase, respectively (Fig. 4A, Supplementary Material, Tables S1 and S2). The total toxin content in exponential growth phase was lowest at salinity treatments 16 and 22 and was higher for both the lower as well as higher salinities. This trend was not observed for stationary growth phase, where only the PST content in cultures maintained at a salinity of 6 was significantly higher (ANOVA, Tukey's HSD test, $p < 0.05$; Supplementary Material, Table S2) compared to all other treatments. Intracellular cyclic imines were found at all salinities (Fig. 4B, Supplementary Material, Tables S1 and S2). The highest cyclic imine content was observed at a salinity of 6 in both the exponential and stationary phase (11–13 pg cell^{-1}). The lowest amount of cyclic imine toxins was observed at a salinity of 22 (3–4 pg cell^{-1}). The cyclic imine toxin quota was largely comparable between both growth phases, and at salinities of 10–34 (5–6 pg cell^{-1}) for the stationary growth phase in particular.

The efficiency of the SPE toxin extraction procedure was tested by determination of the recovery rate of cyclic imines from a solution with a known amount of toxins added. In three independent experiments, 50 mL of pure culture medium was mixed with 150 µL of cyclic imine toxin extracts with known concentrations. The mean recovery rate of all three trials using SPE purification was determined as 98.7 ± 6.3%.

Extracellular cyclic imines were present in all salinity treatments. The extracellular toxin content, expressed as per cell equivalents, ranged between 0.17 pg cell^{-1} at a salinity of 28 and 0.63 pg cell^{-1} at a salinity of 10 for samples of the exponential growth phase (Fig. 4C, Supplementary Material, Table S1). For stationary growth, the amount of extracellular cyclic imines was lower compared to exponential phase and ranged

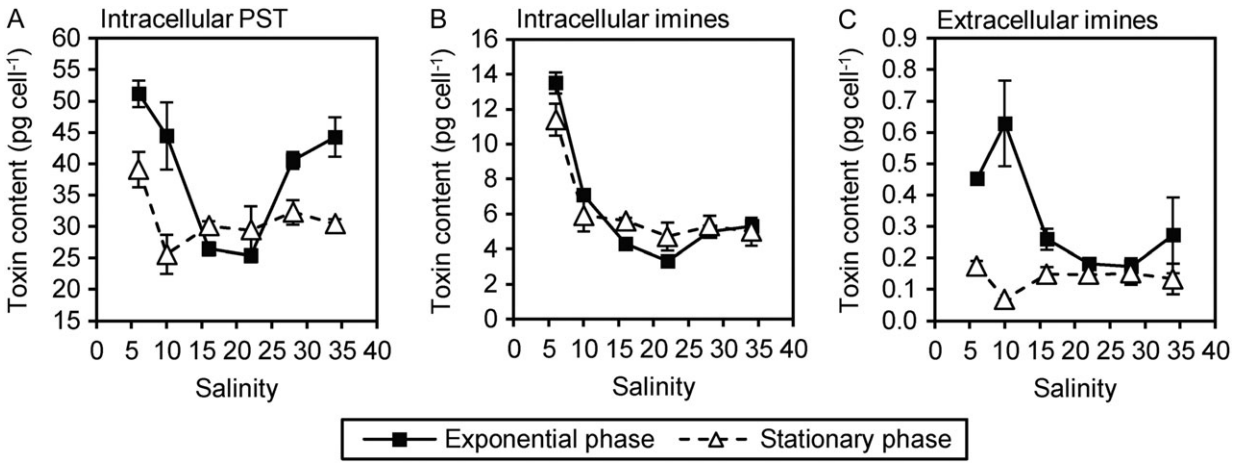

Fig. 4. Toxin content of intracellular PST (**A**), intracellular cyclic imines (**B**) and extracellular cyclic imines (**C**) for triplicate cultures in the exponential and stationary growth phase ($n = 3$, ±1 SD).

between 0.07 pg cell^{-1} at a salinity of 10 and 0.17 pg cell^{-1} at a salinity of 6 (Fig. 4C, Supplementary Material, Table S2). In the exponential growth phase, the extracellular cyclic imines were high for salinities 6 and 10, while for the stationary phase the amounts were generally comparable (but lower at a salinity of 10).

Toxin composition

The qualitative PST profiles were the same for all salinity treatments sampled during exponential and stationary growth phase. All cultures contained C1/C2, B1, STX and GTX2/3. A significant negative correlation (Pearson correlation, $p < 0.05$) was observed between the relative proportions of C1/C2 and STX, both for exponential and stationary phases. At low salinities, the relative amount of C1/C2 was lower than at high salinities. In contrast, the relative amount of STX was highest at low salinities and lowest at high salinities. The relative contribution of GTX2/3 and B1 did not show changes (Fig. 5A, D).

The most abundant cyclic imines were gymnodimine A (GYM), 12-methyl gymnodimine A (12-me GYM) and 13-desmethyl spirolide C (SPX-1). Four other yet undescribed SPX were identified as SPX due to their very characteristic fragmentation pattern in mass spectrometry analysis but, together with 27-hydroxy-13-desmethyl spirolide C, contributed to less than 1% of the total cyclic imines in both growth phases (Supplementary Material, Tables S1 and S2). The relative cellular contents of SPX-1 increased, while GYM decreased, with increasing salinities. Consequently, SPX-1 and GYM were negatively correlated during both growth phases (Pearson correlation, $p < 0.05$; Fig. 5B, E).

The relative amount of total extracellular cyclic imines in relation to the total cyclic imine content varied between 1 to 9%. There was no significant correlation between the amounts of intra- and extracellular cyclic imines. The qualitative composition of cyclic imines found extracellularly was largely comparable to those observed intracellularly (Fig. 5C, F, Supplementary Material, Tables S1 and S2). The extracellular cyclic imines mostly consisted of SPX-1 (40–60%) followed by GYM (20–30%). 12-me GYM was not detected at a salinity of 22 and occurred only in low amounts in the exponential growth phase of the salinity 28 treatment. With relative amounts ranging between 10–20%, the fraction of minor compounds made up a significantly larger fraction of total cyclic imines compared to what was found inside the cells.

Lytic activity

Comparison of culture fractions. For one of the experimental cultures (salinity of 16 in exponential growth phase), a detailed comparison of three fractions (whole culture, supernatant, and cell extract) was performed using high resolution dose–response curves (Supplementary Material, Fig. S2A). Corresponding EC_{50} values (Supplementary Material, Fig. S2B) showed that lytic activity of the cell extract was ca. 6-fold lower and significantly different from the whole cell culture fraction and the supernatant fraction (ANOVA, Tukey's HSD, $p < 0.0001$).

Comparison of salinity treatments. Cell lysis of the target species *R. salina* was observed for all tested salinities (Fig. 6; Supplementary Material, Fig. S3 and S4). For the supernatant fraction in exponential phase at a salinity of 16, only a slight decline of the target species cell count at the highest dose was observed (Supplementary

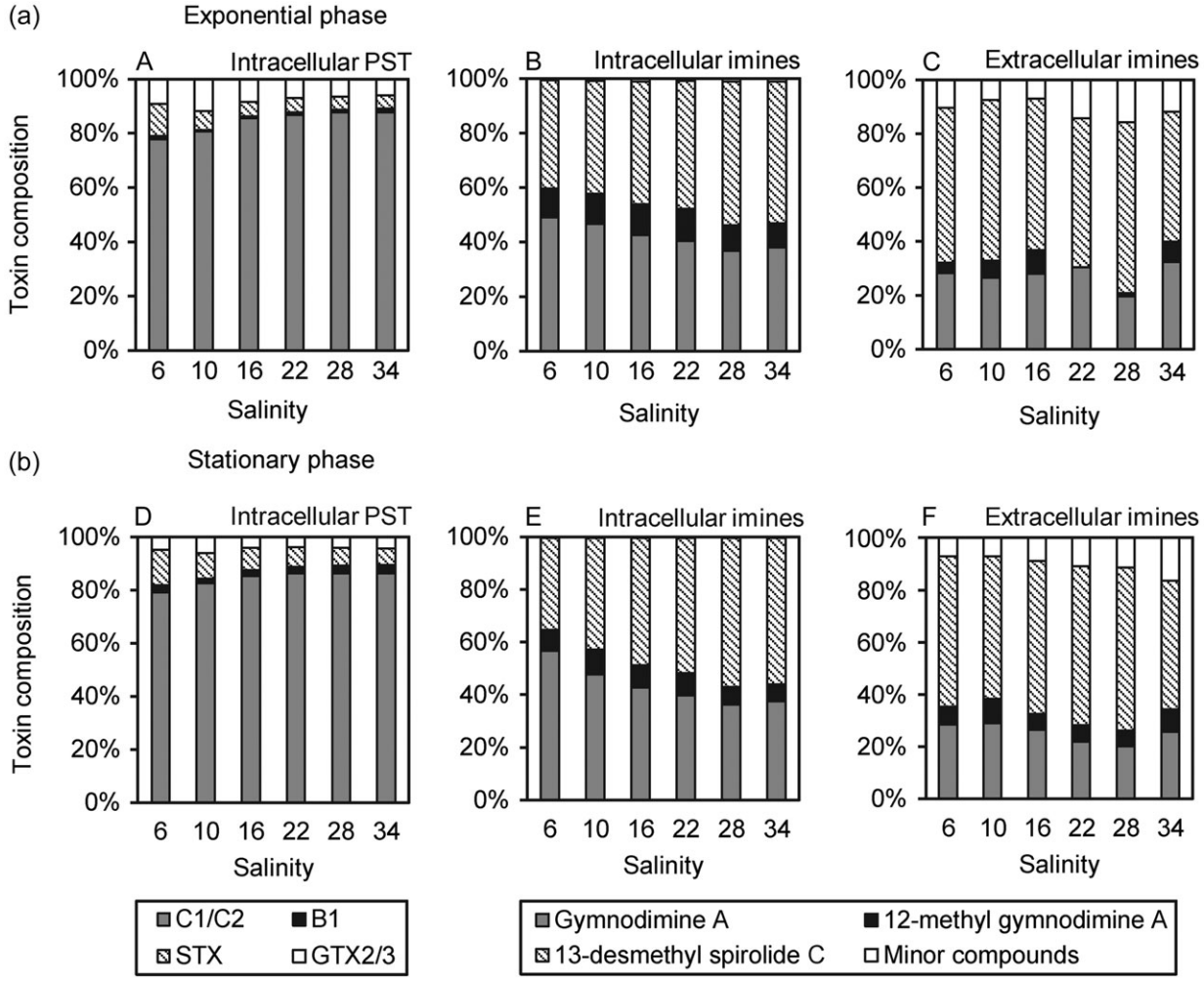

Fig. 5. Toxin composition of intracellular PST (**A**, **D**), intracellular cyclic imines (**B**, **E**) and extracellular cyclic imines (**C**, **F**) for triplicate cultures in the exponential (**a**) and stationary (**b**) growth phases.

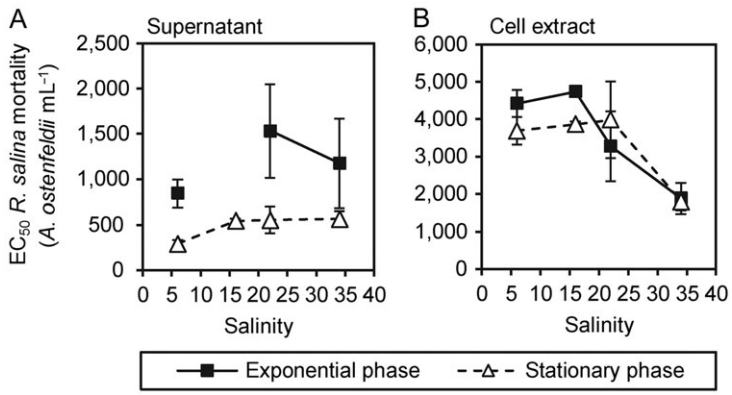

Fig. 6. EC_{50}-values for supernatant (**A**) and cell extract (**B**) of different salinity treatments for the exponential and stationary growth phase. No value is available for the salinity 16 treatment of the supernatant fraction in exponential growth phase. Each data point represents a mean of triplicate cultures ($n = 3$, ± 1 SD).

Material, Fig. S3) and thus no EC_{50}-value could be calculated. For all other treatments, the corresponding EC_{50}-values (Fig. 6) showed that lytic activity of the supernatant fractions were significantly higher (i.e. EC_{50} values were lower) than lytic activity of the cell extract (ANOVA, Tukey's HSD, $p < 0.05$).

Overall, extracellular lytic activity in the stationary phase was higher than in the exponential phase, but as a result of high standard deviations, the differences were not statistically significant (ANOVA, Tukey's HSD, $p > 0.5$). For cell extracts, there was no difference in lytic activity between exponential and stationary phase.

Comparing the different salinities, EC_{50}-values of the supernatant fractions in stationary phase were almost 2-fold lower (i.e. lytic activity was higher) at a salinity of 6 than in the 16, 22 and 34 salinities treatments (ANOVA, Tukey's HSD $p < 0.05$; Supplementary Material, Table S2). Vice versa, in both growth phases the EC_{50}-values of the cell extract fractions at a salinity of 34 were significantly lower (i.e. lytic activity was higher) than in the 22, 16 and 6 salinity treatments (ANOVA, Tukey's HSD $p < 0.05$; Supplementary Material, Table S2).

DISCUSSION

Local *A. ostenfeldii* blooms in the brackish water of the Ouwerkerkse Kreek are exposed to temporally and spatially highly dynamic salinities (Fig. 1B), and this population is therefore expected to be well adapted to a wide range of salinities. Indeed, our results demonstrate a high tolerance of the tested *A. ostenfeldii* clone towards a wide range of salinities with relatively small changes in growth, but dynamic shifts in cell size, elemental composition, toxin production and lytic activity. Although a high intraspecific variability in traits exists within algal populations (Maranda *et al.*, 1985; Burkholder and Glibert, 2006; Alpermann *et al.*, 2010), including the *A. ostenfeldii* population investigated (Van de Waal *et al.*, 2015), we here focussed on a single isolate only in order to accommodate a broad range of variables. The observed responses therefore do not reflect the population response, but provide first insights into putative interactions between growth rate, cell size, toxin synthesis and lytic activity of an *A. ostenfeldii* clone exposed to a range of salinities.

The high capacity of the Dutch *A. ostenfeldii* isolate tested here to grow at all salinities above 4.5 suggests that this population is euryhaline. A barrier for most estuarine planktonic algae at which the organisms suffer extreme osmotic stress is usually observed at a salinity of ~5 (Kies, 1997; Flöder *et al.*, 2010). This is consistent with our observation that cells at a salinity of 3 rapidly died and that at a salinity of 4.5, cells survived but did not grow substantially. However, other plankton species, which are more constantly exposed to very low salinities, can well tolerate salinities at or below 3 (Brand, 1984; Logares *et al.*, 2007; Sjöqvist *et al.*, 2015). Thus, the failure to grow at salinities below 4.5 of the Dutch *A. ostenfeldii* isolate seems to reflect the habitat conditions of the creek. Indeed, salinities in the surface water layer of the Ouwerkerkse Kreek ranged between 8 and 14 during the bloom (Fig. 1). After a heavy rainfall event in mid-August, however, the salinity in the surface layer was reduced to 4, which may have impeded growth and contributed to the bloom collapse. Yet, at the same time, water was pumped out of the creek into the estuary (data not shown) and presumably also contributed to the bloom termination.

Although growth was comparable for all salinities >4.5, slightly higher growth was observed for cultures in salinities ranging from 10 to 22, which are consistent with the growth response of other estuarine and coastal *A. ostenfeldii* isolates (Jensen and Moestrup, 1997; Lim and Ogata, 2005). The salinity optimum of a Baltic *A. ostenfeldii* population was lower and narrower, with optimal growth at salinities ranging from 6 to 10 (Kremp *et al.*, 2009), though Suikkanen *et al.* (2013) reported optimal growth of other isolates from the Baltic Sea at salinities ranging between 6 and 20. Growth over a range of different salinities has also been recorded for *A. ostenfeldii* isolates from marine environments, but saline habitat conditions seem to be reflected by a more narrow salinity tolerance and higher salinities for optimal growth compared to estuarine or brackish water isolates. For instance, optimal growth between salinities of 15–30 was reported for a Danish isolate (Jensen and Moestrup, 1997), and between 25 and 33 for isolates from Nova Scotia, Canada (Maclean *et al.*, 2003). In conclusion, *A. ostenfeldii* generally can be classified as euryhaline but the salinity regime of the habitat seems to play an important role in determining the salinity range of an isolate. Growth at a broad range of different salinities has also been observed for the related species *Alexandrium minutum* (Grzebyk *et al.*, 2003; Lim and Ogata, 2005), which is also known to form dense blooms in harbours, lagoons and other coastal systems (Chang *et al.*, 1997; Hwang and Lu, 2000; Vila *et al.*, 2005).

Cell size of the Dutch *A. ostenfeldii* OKNL21 was affected by salinity. In general, an increase in cell size will reduce the surface area/volume ratio of the cell. Lim and Ogata (2005) speculated that this might enhance the osmoregulation capability of the cell, and therefore possibly allow growth of *A. ostenfeldii* at a broad

salinity range. As predicted, lower salinities resulted in larger cells in both growth phases, probably due to osmosis. Furthermore, enhanced osmoregulation is associated with higher energetic costs, resulting in lower growth rates that may subsequently lead to larger cell sizes. We currently do not have a conclusive explanation as to why cells in stationary phase remained smaller at higher salinities. This may have been caused by increased gamete formation at higher salinities, as gametes are generally smaller than normal vegetative cells. Further studies are required to elucidate the putative role of salinity in transition events of the *A. ostenfeldii* life cycle, as formation of resting cysts as seeding stocks for the next season is important for the persistence of annual recurrent blooms.

Salinity did not affect cell yield, i.e. the maximum cell density at stationary phase, which for all treatments was ~10 000 cells mL^{-1}. Organic N and P build-up amounted to 330 µM N and 19 µM P, respectively, and with 465 µM N and 18 µM P in the medium, phosphate likely became limiting. Yet, the elemental ratios did not indicate severe limitation by nutrients, as these were generally close to the Redfield ratio C:N:P of 106:16:1 (Redfield, 1934, 1958). Limitation by inorganic carbon or an effect of higher pH may also have caused growth cessation (Hansen, 2002; Pedersen and Hansen, 2003). Interestingly, at both the lowest and highest salinities, C:N, C:P and N:P ratios were higher than the Redfield ratio, notably in the stationary phase. These higher ratios resulted from higher cellular N, but particularly higher cellular C quota. Such higher C and N quota may, in turn, be associated with salinity driven shifts towards larger cell sizes and consequently higher investments in cell walls. Indeed, cell walls typically consist of polysaccharides and proteoglycans (Domozych, 2011), which are rich in C and N (Sterner and Elser, 2002). Thus, salinity may have consequences for the biochemical make-up of cells, and thereby alter the elemental composition towards particularly higher C:N and C:P ratios.

Generally, growth rates of the tested *A. ostenfeldii* strain OKNL21 were low, and at the lower end of the range of growth rates (between 0.2 and 0.3 d^{-1}) reported for other *A. ostenfeldii* strains (Jensen and Moestrup, 1997; Maclean *et al.*, 2003). Relatively slow growth, but the ability to form dense blooms, clearly indicates that *A. ostenfeldii* is very successful in reducing grazing loss and in outcompeting other fast-growing phytoplankton species. It is tempting to speculate that the broad cocktail of bioactive compounds of the Dutch *A. ostenfeldii* population plays an important role in this respect. For instance, PST may play a role in deterring copepod grazers (Bagoien *et al.*, 1996; Teegarden and Cembella, 1996; Selander *et al.*, 2006), and the deleterious effect of extracellular lytic compounds towards accompanying protists (Tillmann and John, 2002; Tillmann *et al.*, 2007; Tillmann and Hansen 2009) clearly supports *A. ostenfeldii* bloom formation.

Our results show up to a 2-fold increase of PST and cyclic imine toxin quota at the lower and higher salinities compared to intermediate salinities of 16 and 22 (Fig. 4A, B). These changes seem to be associated to shifts in growth rates, and particularly accompanied to shifts towards larger cell sizes. Indeed, PST quota showed a significant negative correlation with growth rate (Pearson correlation, $r = -0.49$, $p < 0.05$; Fig. 7), and a significant positive correlation with cell volume (Pearson correlation, $r = 0.63$, $p < 0.05$; Fig. 7) in exponential growth phase. Specifically, toxin quota seems to be flexible only at larger cell volumes, with quotas of ~30 pg $cell^{-1}$ for PST and 5 pg $cell^{-1}$ for cyclic imines at smaller volumes (Fig. 7C, D). Whether these minimum toxin quotas are constraint by cell volume, or result from direct salinity effects remains to be elucidated. The higher toxin quota at the lowest growth rate may possibly result from accumulation of toxins in the cells and has been reported earlier for various *Alexandrium* species, though this relationship depends strongly on the growth-controlling factors (Anderson *et al.*, 1990; Cembella, 1998; Van de Waal *et al.*, 2013). Either way, our results demonstrate a clear yet complex coupling between salinity and *A. ostenfeldii* growth rate, cell size and toxin synthesis.

Cultures of OKNL21 at low salinities produced a higher amount of STX while cultures at higher salinities produced more C1/C2 toxins. STX is the most toxic PST with an equivalent toxicity of 2045 mouse units per µmol. In comparison, the C-toxins are distinctly less toxic (20–300 MU $µmol^{-1}$) (Genenah and Shimizu, 1981). It is unclear why PST quota, and in particular STX, is higher at the lowest salinity. Whether this is a result of the minor changes in growth rate, of shifts in cell size, or due to a potential role of these toxins in osmoregulation remains to be elucidated. Comparable to the shift from C1/C2 to STX, there were also salinity-dependent shifts in the ratio of single cyclic imine toxins. More specifically, *A. ostenfeldii* OKNL21 produced a higher amount of gymnodimine A at low salinities or, respectively, a higher amount of 13-desmethyl spirolide C if the salinity was high. Such salinity-dependent shifts in production of different cyclic imine toxins were also found for *A. ostenfeldii* SPX by Otero *et al.* (2010). Thus, environmental factors can influence the toxin composition of *A. ostenfeldii* for both toxin groups (i.e. PST and spiroimines), though the underlying physiological and metabolic mechanisms remain unknown.

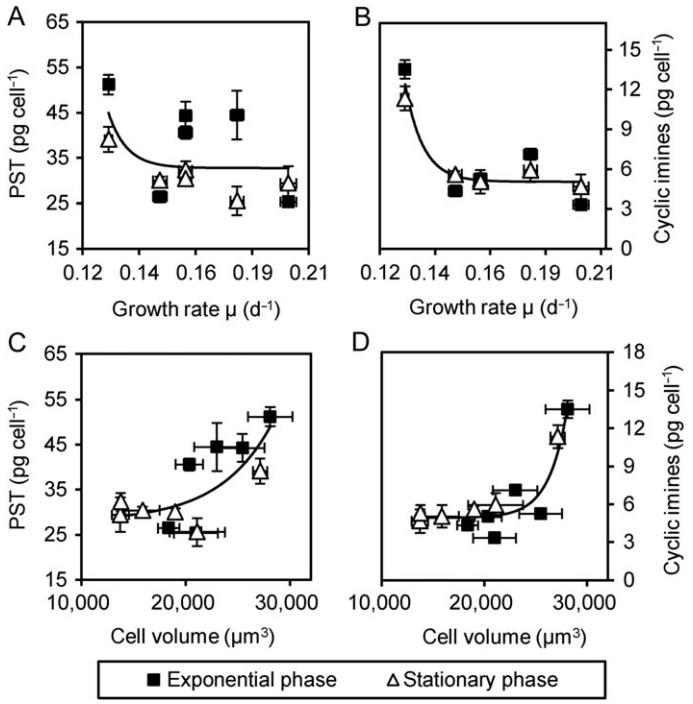

Fig. 7. Toxin content for PST and cyclic imines versus growth rate (**A**, **B**) and cell volume (**C**, **D**) for triplicate cultures in the exponential and stationary growth phase ($n = 3$, ±1 SD). Solid black lines indicate a significant ($p < 0.05$) three parameter exponential regression through all data points.

In order to follow the hypothesis of an osmotic stress induced increase of extracellular organic compounds in *A. ostenfeldii*, we also intended to detect and quantify the extracellular toxins. Whereas an initial attempt to quantify extracellular PST using SPE or solid phase adsorption toxin tracking using HP-20 resins failed because of low recovery (unpublished data), recovery of a known amount of added dissolved cyclic imine toxins with SPE extraction was close to 100%. Overall, total cyclic imine concentrations were ~10-fold higher inside the cells than were measured extracellularly, while qualitative toxin composition remained largely unaltered for the major compounds (Fig. 5). The proportions of extracellular minor compounds relative to intracellular minor compounds were ~15-fold higher in the exponential growth phase, and 20-fold higher in the stationary growth phase (Fig. 4B-F). This may suggest that some of these minor compounds are rapidly metabolized inside but not outside the cells, or that some of these compounds are the product of extracellular (e.g. bacterial) degradation or metabolic processes.

The distinct differences between intra- and extracellular concentrations of total cyclic imines suggest that these compounds are primarily intracellular metabolites and thus provide no evidence for a role as extracellular compounds. Yet, we cannot exclude that the molecules, when released into the environment, become undetectable either because of binding to target sites or because of bacteria induced bio-transformation and/or degradation. Extracellular cyclic imine concentrations were generally higher during the exponential phase compared to the stationary phase, particularly at lower salinities, which might indicate an increased excretion of these compounds by actively growing cells. Alternatively, however, this may also reflect an increased degradation in older cultures as bacterial densities usually peak when algal cultures become dense. At low salinities, the extracellular cyclic imine toxin content in exponential phase was up to 2-fold higher than it was observed for higher salinities. Enhanced osmotic stress at low salinities presumably caused the higher amount of extracellular cyclic imine toxin concentrations, regardless of being the result of active excretion or passive release by disturbed osmoregulation.

The majority of lytic compounds produced by *A. ostenfeldii* OKNL21 is excreted and acting extracellularly, underlining a rather unspecific role of allelochemical compounds in grazer impairment and competition (Tillmann and John, 2002; Tillmann *et al.*, 2007). The lytic activity of cell free supernatant at a salinity of 6 was substantially higher than samples at any other salinity. Similar to the cyclic imines, it is conceivable that an enhanced osmotic stress at this lowest salinity caused a higher amount of extracellular lytic compounds, regardless of being caused by an active excretion or a more passive release as a result of disturbed osmoregulation. In contrast, at high salinity (e.g. salinity 34) an

accumulation of lytic compounds was observed in the cells. It thus seems that there is a difference in release or accumulation of lytic compounds depending on salinity and osmotic stress.

CONCLUSION

Our results demonstrate a broad salinity range at which optimal growth of *A. ostenfeldii* OKNL21 was largely maintained, but also that at salinities below 6, growth ceases. Cell sizes were generally higher both at the lowest and highest salinities, and were accompanied by increased cellular content of bioactive compounds including PST and cyclic imine toxins, particularly at lowest salinities. Furthermore, the production and excretion of lytic compounds seemed to increase and decrease, respectively, with increasing salinities. Such dynamic changes in the cellular production and excretion of toxic and allelochemical compounds indicate a high resilience of this population to salinity variations. We also show that blooms of *A. ostenfeldii* can potentially be prevented when salinities remain below 6, and our results may thus support future management decisions.

SUPPLEMENTARY DATA

Supplementary data can be found online at http://plankt.oxfordjournals.org.

ACKNOWLEDGEMENT

We greatly acknowledge technical assistance by Anne Müller and Wolfgang Drebing.

FUNDING

This work was supported by the PACES research programme of the Alfred Wegener Institute as part of the Helmholtz Foundation initiative in Earth and Environment. The work of KMB is funded by the Gieskes-Strijbis Foundation.

REFERENCES

Alpermann, T. J., Tillmann, U., Beszteri, B., Cembella, A. D. and John, U. (2010) Phenotypic variation and genotypic diversity in a planktonic population of the toxigenic marine dinoflagellate *Alexandrium tamarense* (Dinophyceae). *J. Phycol.*, **46**, 18–32.

Anderson, D. M., Kulis, D. M., Sullivan, J. J., Hall, S. and Lee, C. (1990) Dynamics and physiology of saxitoxin production by the dinoflagellates *Alexandrium* spp. *Mar. Biol.*, **104**, 511–524.

Anderson, D. M., Alpermann, T. J., Cembella, A. D., Collos, Y., Masseret, E. and Montresor, M. (2012) The globally distributed genus *Alexandrium*. Multifaceted roles in marine ecosystems and impacts on human health. *Harmful Algae*, **14**, 10–35.

Bagoien, E., Miranda, A., Reguera, B. and Franco, J. M. (1996) Effects of two paralytic shellfish toxin producing dinoflagellates on the pelagic harpacticoid copepod *Euterpina acutifrons*. *Mar. Biol.*, **126**, 361–369.

Borkman, D. G., Smayda, T. J., Tomas, C. R., York, R., Strangman, W. and Wright, J. L. (2012) Toxic *Alexandrium peruvianum* (Balech and de Mendiola) Balech and Tangen in Narragansett Bay, Rhode Island (USA). *Harmful Algae*, **19**, 92–100.

Brand, L. E. (1984) The salinity tolerance of forty-six marine phytoplankton isolates. *Estuar. Coast. Shelf Sci.*, **18**, 543–556.

Burkholder, J. M. and Glibert, P. M. (2006) Intraspecific variability: an important consideration in forming generalisations about toxigenic algal species. *Afr. J. Mar. Sci.*, **28**, 177–180.

Burson, A., Matthijs, H. C., Bruijne, W., de Talens, R., Hoogenboom, R. and Gerssen, A. *et al.* (2014) Termination of a toxic *Alexandrium* bloom with hydrogen peroxide. *Harmful Algae*, **31**, 125–135.

Cembella, A. D. (1998) Ecophysiology and metabolism of paralytic shellfish toxins in marine microalgae. In: Anderson, D. M., Cembella, A. D. and Hallegraeff, G. M. *Physiological Ecology of Harmful Algal Blooms*. Springer Verlag, Berlin. pp. 381–403.

Cembella, A. and Krock, B. (2008) Cyclic imine toxins: chemistry, biogeography, biosynthesis and pharmacology. In: and Botana, L. *Seafood and Freshwater Toxins*. CRC Press, Boca Raton, FL. pp. 561–580.

Chang, F., Anderson, D. M., Kulis, D. M. and Till, D. G. (1997) Toxin production of *Alexandrium minutum* (Dinophyceae) from the Bay of Plenty, New Zealand. *Toxicon.*, **35**, 393–409.

Domozych, D. S. (2011) Algal cell walls. *Encyclopedia of Life Sciences*. John Wiley & Sons, London, New York.

Flöder, S., Jaschinski, S., Wells, G. and Burns, C. W. (2010) Dominance and compensatory growth in phytoplankton communities under salinity stress. *J. Exp. Mar. Biol. Ecol.*, **395**, 223–231.

Genenah, A. A. and Shimizu, Y. (1981) Specific toxicity of paralytic shellfish poisons. *J. Agric. Food Chem.*, **29**, 1289–1291.

Grzebyk, D., Béchemin, C., Ward, C. J., Vérite, C., Codd, G. A. and Maestrini, S. Y. (2003) Effects of salinity and two coastal waters on the growth and toxin content of the dinoflagellate *Alexandrium minutum*. *J. Plankton Res.*, **25**, 1185–1199.

Hakanen, P., Suikkanen, S., Franzén, J., Franzén, H., Kankaanpää, H. and Kremp, A. (2012) Bloom and toxin dynamics of *Alexandrium ostenfeldii* in a shallow embayment at the SW coast of Finland, northern Baltic Sea. *Harmful Algae*, **15**, 91–99.

Hansen, P. J. (2002) Effect of high pH on the growth and survival of marine phytoplankton: implications for species succession. *Aquat. Microb. Ecol.*, **28**, 279–288.

Hwang, D. F. and Lu, Y. H. (2000) Influence of environmental and nutritional factors on growth, toxicity, and toxin profile of dinoflagellate *Alexandrium minutum*. *Toxicon*, **38**, 1491–1503.

Jensen, M. Ø. and Moestrup, Ø. (1997) Autecology of the toxic dinoflagellate *Alexandrium ostenfeldii*. Life history and growth at different temperatures and salinities. *Eur. J. Phycol.*, **32**, 9–18.

Keller, M. D., Selvin, R. C., Claus, W. and Guillard, R. R. L. (1987) Media for the culture of oceanic ultraphytoplankton. *J. Phycol.*, **23**, 633–638.

Kies, L. (1997) Distribution, biomass and production of planktonic and benthic algae in the Elbe Estuary. *Oceanograph. Lit. Rev.*, **11**, 1328.

Kremp, A., Lindholm, T., Dreßler, N., Erler, K., Gerdts, G., Eirtovaara, S. and Leskinen, E. (2009) Bloom forming *Alexandrium ostenfeldii* (Dinophyceae) in shallow waters of the Åland Archipelago, Northern Baltic Sea. *Harmful Algae*, **8**, 318–328.

Kremp, A., Tahvanainen, P., Litaker, W., Krock, B., Suikkanen, S. and Leaw, C. P. *et al.* (2014) Phylogenetic relationships, morphological variation, and toxin patterns in the *Alexandrium ostenfeldii* (Dinophyceae) complex: implications for species boundaries and identities. *J. Phycol.*, **50**, 81–100.

Lim, P.-T. and Ogata, T. (2005) Salinity effect on growth and toxin production of four tropical *Alexandrium* species (Dinophyceae). *Toxicon*, **45**, 699–710.

Logares, R., Rengefors, K., Kremp, A., Shalchian-Tabrizi, K., Boltkovskoy, A., Tengs, T., Shurtleff, A. and Klaveness, D. (2007) Phenotypically different microalgal morphospecies with identical ribosomal DNA: a case of rapid adaptive evolution?. *Microb. Ecol.*, **53**, 549–561.

Ma, H., Krock, B., Tillmann, U. and Cembella, A. (2009) Preliminary characterization of extracellular allelochemicals of the toxic marine dinoflagellate *Alexandrium tamarense* using a *Rhodomonas salina* bioassay. *Mar. Drugs*, **7**, 497–522.

Maclean, C., Cembella, A. D. and Quilliam, M. A. (2003) Effects of light, salinity and inorganic nitrogen on cell growth and spirolide production in the marine dinoflagellate *Alexandrium ostenfeldii* (Paulsen) Balech et Tangen. *Bot. Mar.*, **46**, 466–474.

Maranda, L., Anderson, D. M. and Shimizu, Y. (1985) Comparison of toxicity between populations of *Gonyaulax tamarensis* of Eastern North American waters. *Estuar. Coast. Shelf Sci.*, **24**, 401–410.

Otero, P., Alfonso, A., Vieytes, M. R., Cabado, A. G., Vieites, J. M. and Botana, L. M. (2010) Effects of environmental regimens on the toxin profile of *Alexandrium ostenfeldii*. *Environ. Toxicol. Chem.*, **29**, 301–310.

Pedersen, F. M. and Hansen, P. J. (2003) Effects of high pH on the growth and survival of six marine heterotrophic protists. *Mar. Ecol. Prog. Ser.*, **260**, 33–41.

Redfield, A. C. (1934) On the proportions of organic derivatives in sea water and their relation to the composition of plankton. In Daniel, R. J. (ed.) *James Johnstone Memorial Volume*. University Press of Liverpool, Liverpool, UK, pp. 177–192.

Redfield, A. C. (1958) The biological control of chemical factors in the environment. *Am. Sci.*, **46**, 205–221.

Salgado, P., Riobó, P., Rodríguez, F., Franco, J. M. and Bravo, I. (2015) Differences in the toxin profiles of *Alexandrium ostenfeldii* (Dinophyceae) strains isolated from different geographic origins: evidence of paralytic toxin, spirolide, and gymnodimine. *Toxicon*, **103**, 85–98.

Selander, E., Thor, P., Toth, G. and Pavia, H. (2006) Copepods induce paralytic shellfish toxin production in marine dinoflagellates. *Proc. Biol. Sci.*, **273**, 1673–1680.

Shimizu, Y. (1996) Microalgal metabolites: a new perspective. *Annu. Rev. Microbiol.*, **50**, 431–465.

Sjöqvist, C., Godhe, A., Jonsson, P. R., Sundqvist, L. and Kremp, A. (2015) Local adaptation and oceanographic connectivity pattern explain genetic differentiation of a marine diatom across the North Sea–Baltic Sea salinity gradient. *Mol. Ecol.*, **24**, 2871–2885.

Stefels, J. (2000) Physiological aspects of the production and conversion of DMSP in marine algae and higher plants. *J. Sea Res.*, **43**, 183–197.

Sterner, R. W. and Elser, J. J. (2002) *Ecological Stoichiometry: The Biology of Elements from Molecules to the Biosphere*. Princeton University Press, Princeton, USA.

Stolte, W., Panosso, R., Gisselson, L. A. and Granéli, E. (2002) Utilization efficiency of nitrogen associated with riverine dissolved organic carbon (>1kDa) by two toxin-producing phytoplankton species. *Aquat. Microbiol. Ecol.*, **29**, 97–105.

Suikkanen, S., Kremp, A., Hautala, H. and Krock, B. (2013) Paralytic shellfish toxins or spirolides? The role of environmental and genetic factors in toxin production of the *Alexandrium ostenfeldii* complex. *Harmful Algae*, **26**, 52–59.

Teegarden, G. J. and Cembella, A. D. (1996) Grazing of toxic dinoflagellates, *Alexandrium* spp., by adult copepods of coastal maine: implications for the fate of paralytic shellfish toxins in marine food webs. *J. Exp. Mar. Biol. Ecol.*, **196**, 145–176.

Tillmann, U. and Hansen, P. J. (2009) Allelopathic effects of *Alexandrium tamarense* on other algae: evidence from mixed growth experiments. *Aquat. Microb. Ecol.*, **57**, 101–112.

Tillmann, U. and John, U. (2002) Toxic effects of *Alexandrium* spp. on heterotrophic dinoflagellates: an allelochemical defence mechanism independent of PSP-toxin content. *Mar. Ecol. Prog. Ser.*, **230**, 47–58.

Tillmann, U., John, U. and Cembella, A. (2007) On the allelochemical potency of the marine dinoflagellate *Alexandrium ostenfeldii* against heterotrophic and autotrophic protists. *J. Plankton Res.*, **29**, 527–543.

Tillmann, U., Alpermann, T. L., da Purificação, R. C., Krock, B. and Cembella, A. (2009) Intra-population clonal variability in allelochemical potency of the toxigenic dinoflagellate *Alexandrium tamarense*. *Harmful Algae*, **8**, 759–769.

Tomas, C. R., van Wagoner, R., Tatters, A. O., White, K. D., Hall, S. and Wright, J. L. (2012) *Alexandrium peruvianum* (Balech and Mendiola) Balech and Tangen a new toxic species for coastal North Carolina. *Harmful Algae*, **17**, 54–63.

Van de Waal, D., Tillmann, U., Zhu, M., Koch, B., Rost, B. and John, U. (2013) Nutrient resupply induces dynamic changes in C:N:P stoichiometry, amino acid composition and PSP toxin production in *Alexandrium tamarense*. *Mar. Ecol. Prog. Ser.*, **493**, 57–69.

Van de Waal, D. B., Tillmann, U., Martens, H., Krock, B., van Scheppingen, Y. and John, U. (2015) Characterization of multiple isolates from an *Alexandrium ostenfeldii* bloom in The Netherlands. *Harmful Algae*, **49**, 94–104.

van Wagoner, R. M., Misner, I., Tomas, C. R. and Wright, J. L. (2011) Occurrence of 12-methylgymnodimine in a spirolide-producing dinoflagellate *Alexandrium peruvianum* and the biogenetic implications. *Tetrahedron Lett.*, **52**, 4243–4246.

Vila, M., Giacobbe, M. G., Masó, M., Gangemi, E., Penna, A. and Sampedro, N. *et al.* (2005) A comparative study on recurrent blooms of *Alexandrium minutum* in two Mediterranean coastal areas. *Harmful Algae*, **4**, 673–695.